



Open access

2,361 39

Views | CrossRef citations to date | Altmetric

0

[Listen](#)

Articles

Applicability of connectionist methods to predict dynamic viscosity of silver/water nanofluid by using ANN-MLP, MARS and MPR algorithms

Mohammad Hossein Ahmadi , Behnam Mohseni-Gharyehsafa,
Mahmood Farzaneh-Gord, Ravindra D. Jilte, Ravinder Kumar & Kwok-wing Chau

Pages 220-228 | Received 02 Dec 2018, Accepted 15 Jan 2019, Published online: 05 Mar 2019

Cite this article <https://doi.org/10.1080/19942060.2019.1571442>



Full Article

Figures & data

References

Citations

Metrics

Licensing

Reprints & Permissions

View PDF

View EPUB

Share

Formulae display: **MathJax**

ABSTRACT

Dynamic viscosity considerably affects the heat transfer and flow of fluids. Due to improved thermophysical properties of fluids containing nanostructures, these types of fluids are widely employed in thermal mediums. The nanofluid's dynamic viscosity relies on different variables including size of solid phase, concentration and temperature. In the present study, three algorithms including multivariable polynomial regression (MPR), artificial neural network-multilayer perceptron (ANN-MLP) and multivariate adaptive regression splines (MARS) are applied to model the dynamic viscosity of silver (Ag)/water nanofluid. Recently published experimental investigations

process to be the most important ones are the size of particles, fluid temperature and the concentration of Ag nanoparticles in the base fluid. The R^2 values for the studied models are 0.9998, 0.9997 and 0.9996 for the ANN-MLP, MARS and MPR algorithms, respectively. In addition, based on importance analysis, the temperature is highly effective and the dominant parameter for the dynamic viscosity of the nanofluid in comparison with size and concentration.

KEYWORDS:

- [nanofluid](#)
- [dynamic viscosity](#)
- [artificial neural network](#)
- [concentration](#)
- [multivariate adaptive regression splines \(MARS\)](#)
- [multivariable polynomial regression \(MPR\)](#)

Nomenclature

φ	=	Concentration
T	=	Temperature (°C)
d	=	Size (nm)
μ	=	Dynamic viscosity
a_i	=	Coefficients in MPR method
b_i	=	Coefficients in MARS method
BF	=	Basic function (MARS method)

GCV	=	Generalized cross-validation
AAPRE	=	Average absolute percent relative error
RMSE	=	Root mean square error
R2	=	Coefficient of determination
MARS	=	Multivariate adaptive regression splines
MPR	=	Multivariable polynomial regression
ANN	=	Artificial neural network
MLP	=	Multilayer perceptron
C(M)	=	Complexity penalty

1. Introduction

Nano-sized materials such as nanosheets or nanoparticles can be dispersed in a base fluid to prepare nanofluids (Ahmadi, Mirlohi, Nazari, & Ghasempour, [2018](#); Nazari, Ghasempour, Ahmadi, Heydarian, & Shafii, [2018](#)). According to the literature, nanofluids, due to adjustable properties and high stable dispersion, may be used in various applications, including cooling in engines, lubrication, solar water heating, etc. Moreover, one of the major points of nanofluids is their application in thermal systems to enhance the heat transfer rate (Ramezanizadeh, Albuvi Nazari, Ahmadi, & Chau,

[2015](#)). The higher and improved heat transfer rate obtained from utilizing these materials owe to thermophysical properties such as their thermal conductivity. Adding nanostructures into the base fluid influences the dynamic viscosity, specific heat, etc. The dependency of thermophysical properties on various parameters such as temperature, synthesis procedure, pH and concentration is investigated in several pieces of research (Baghban, Jalali, Shafiee, Ahmadi, & Chau, [2019](#); Hosseini, Kasaeian, Pourfayaz, Sheikhpour, & Wen, [2018](#); Zeinali Heris, Kazemi-Beydokhti, Noie, & Rezvan, [2012](#)).

The dynamic viscosity of nanofluids significantly affects their fluid flow and heat transfer (Ahmadi et al., [2018](#); Ebrahimi-Moghadam, Mohseni-Gharyehsafa, & Farzaneh-Gord, [2018](#); Mohseni-Gharyehsafa et al., [2018](#); Nazari, Ahmadi, Ghasempour, & Shafii, [2018](#)). Given this fact, it is critical to get better awareness of the parameters affecting this property. According to the literature review, an increase in temperature results in lower dynamic viscosity, which facilitates fluid motion due to the reduction in friction. Another effective factor in dynamic viscosity is the concentration of nanostructures dispersed in the base fluid (Chiam, Azmi, Usri, Mamat, & Adam, [2017](#); Soltani & Akbari, [2016](#)). On the basis of the results of experimental studies, an increase in concentration leads to an improvement of dynamic viscosity (Asadi & Asadi, [2016](#)). The size of nanostructures plays a key role in thermophysical properties of nanofluids.

Artificial neural networks are widely employed for modeling the system and pattern recognition. Artificial neural networks are applicable in modeling the thermophysical properties of nanofluids (Ahmadi, Tatar, Nazari, Mahian, & Ghasempour, [2018](#); Chau, [2017](#); Kazemi et al., [2018](#); Rezaei, Sadeghzadeh, Alhuyi Nazari, Ahmadi, & Astarai, [2018](#)). Ahmadi et al. ([2018](#)) employed the least square support vector machine (LSSVM) and group method of data handling (GMDH) approaches to model the thermal conductivity value of CuO/EG (Copper-Oxide/Ethylene-Glycol) nanofluid. It was monitored from the outcomes that the R^2 values for GMDH and LSSVM were equal to 0.994 and 0.991, respectively. These values indicated the high accuracy of the models in estimating the nanofluid's thermal conductivity. In another piece of research (Ahmadi et al., [2018](#)), LSSVM was employed to predict the thermal conductivity of alumina/EG. The R^2 value for the proposed model was 0.9902. In another investigation, Baghban et al. ([2018](#)) used seven intelligent models to seek the relationship between coefficients of the convective heat transfer of silica nanoparticles as a function of three independent parameters including mass fraction, Prandtl number and Reynolds number. Statistical

criteria show that the committee machine intelligent system (CMIS) has the highest accuracy with an R^2 of 0.997.

To propose a estimation tool, it is essential to consider the factors influencing the output data (Ahmadi et al., [2018](#)). Most studies consider temperature and concentration when modeling thermophysical properties; adding size as another input variable results in more accurate results. In the current study, the Ag/water nanofluid's dynamic viscosity is modeled by applying MPR, ANN-MLP and MARS algorithms. The input variables in the modeling process are temperature, size and volumetric concentration.

2. Intelligent modes

2.1. Multilayer perceptron neural network

Artificial neural networks are conventionally applied for prediction purposes. MLP is a feed-forward neural network algorithm. This network is composed of an input layer, hidden layer and output layer (Gardner & Dorling, [1998](#); Hornik, Stinchcombe, & White, [1989](#)). The number of input and output layers depends on the data. In the hidden layer, one or more layers can exist that have various neurons (Orhan, Hekim, & Ozer, [2011](#)). In these types of neural networks, the initial neuron of the layer is fed into the neuron of layer in the next stage, which is the same for all layers except the first layer. Each neuron has an activation function and a sum function. The inputs are initially multiplied by the weighting factor and added to each other. Afterwards, a bias factor is added to the calculated number. In the next step, the number obtained from the summing function is used in the activation function as input data. Activation functions are categorized in three forms as represented below, where ϕ is the activation function (Ruck, Rogers, Kabrisky, Oxley, & Suter, [1990](#); Vanzella et al., [2004](#)).

$\phi(r) = \exp(-r^2 / 2\sigma^2)$ (1) In the above equation, $\sigma > 0$ is the width, which shows the interpolating function smoothness. The distance between x and the center is defined by r .

Trial and error steps or intelligent approaches may be employed in order to calculate the number of layers. The optimum condition is obtained based on the Mean Square Error (MSE) parameter; therefore, these steps are performed to achieve the ideal status

accurate number of steps must be considered (Goda, Shokir, Eissa, Fattah, & Sayyounh, [2003](#)).

2.2. Multivariate adaptive regression splines

MARS is applied in regression and data classification (Friedman & Roosen, [1995](#)). This approach is mainly utilized to predict the dependent data, Y ($n \times 1$), which are continuous, based on the group of input data ($n \times p$). This model is represented as follows:

$$y=f(x)+e \quad (2)$$

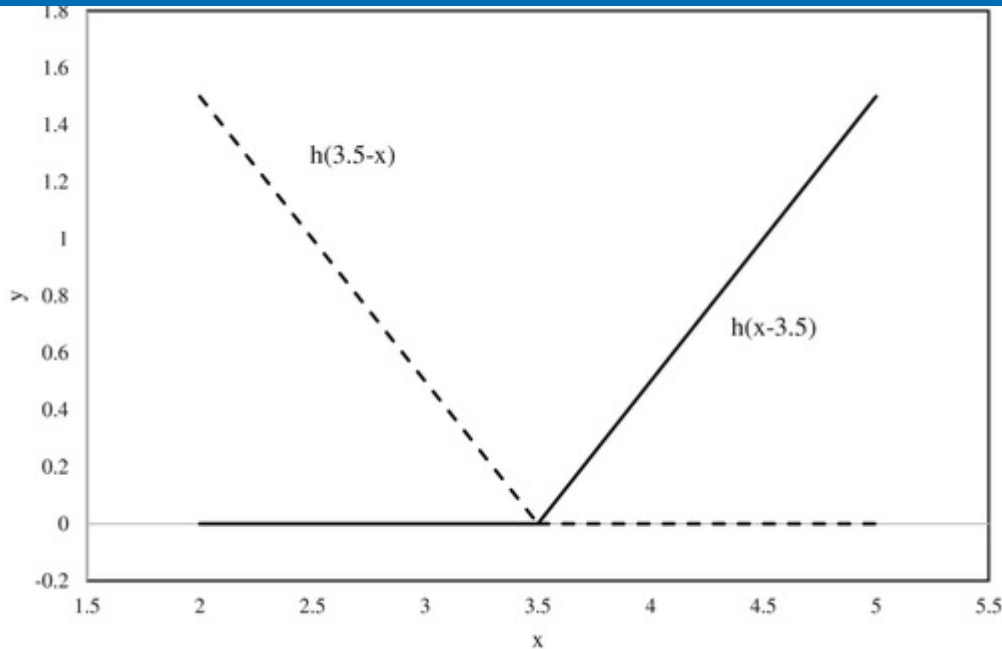
In the above equation, f indicates the weighted sum of basic functions. These functions are dependent on X . In addition, e stands for the error, which is an ($n \times 1$) matrix. In this method, no priori assumption is required for estimating the relationship between dependent and independent data. The relationship between these data is found on the basis of a group of coefficients and piecewise polynomials. The model is generated using this algorithm based on fitting basic functions to independent variables' distinct intervals. Typically, the polynomials that are called "splines" consist of pieces connecting to each other. The connecting points of the splines are known as "nodes," "knots" or "breakdown points." The points are shown by t . In a q -degree spline, each section is a polynomial function. The function utilized by the MARS algorithm is described as:

$$[-(x-t)]_+^q = (t-x)^q \text{ if } x < t \quad 0 \text{ otherwise} \quad (3)$$

$$[+(x-t)]_+^q = (x-t)^q \text{ if } x \geq t \quad 0 \text{ otherwise} \quad (4)$$

In the above equation, q (≥ 0) is the power at which the splines are boosted up. The smoothness of the obtained function depends on the value of q . In the case of $q = 1$, as in the present study, just simple linear splines are applied. In Figure 1, a pair of splines for the node $t = 3.5$ is shown.

Figure 1. Spline at $t = 3.5$ (Nieto, García-Gonzalo, Bernardo Sanchez, & Menendez Fernandez, [2016](#)).



Display full size

By considering y which has M basis functions, the model proposed by MARS can be written (Chou, Lee, Shao, & Chen, [2004](#); De Cos Juez, Lasheras, García Nieto, & Suárez, [2009](#); Friedman & Roosen, [1995](#); Nieto & Antón, [2014](#); Nieto, Fernández, Lasheras, de Cos Juez, & Muñiz, [2012](#); Nieto, Lasheras, de Cos Juez, & Fernández, [2011](#); Orhan et al., [2011](#); Xu et al., [2004](#)) as:

$\hat{y} = f^M(x) = c_0 + \sum_{m=1}^M c_m B_m(x)$ (5) \hat{y} indicates the parameter predicted by MARS, c_0 is a fixed value, the m th basis function is referred to as $B_m(x)$ and c_m refers to the m th basis function's coefficient. It is crucial to optimize the variables (c_0 and c_m) announced into the knot positions and the model. For a dataset of X which has n objects and p input variables, $N = n \times p$ pairs of spline basic functions exist which can be calculated using Equations (3) and (4). In order to generate the final model, a two-step process must be followed. In the first stage, a two-at-a-time forward stepwise process is performed to choose the basis functions (Chou et al., [2004](#); De Cos Juez et al., [2009](#); Friedman & Roosen, [1995](#); Nieto & Antón, [2014](#); Nieto et al., [2012](#); Nieto et al., [2011](#); Orhan et al., [2011](#); Xu et al., [2004](#)). Using this procedure for selection leads to a model with inappropriate ability to predict new data due to the complexity and overfitting of the model. In order to enhance this ability, the redundant basis functions may be removed by applying a backward stepwise procedure. In order to select the usable functions, GCV is utilized (Chou et al., [2004](#); De Cos Juez et al., [2009](#); Friedman & Roosen, [1995](#); Nieto & Antón, [2014](#); Nieto et al., [2012](#), [2011](#); Orhan et al., [2011](#); Xu et al., [2004](#)). In this approach, the GCV is defined as the average squared residual error

divided by a penalty based on the complexity of the model. The GCV is calculated as follows:

$$\text{GCV}(M) = \frac{1}{n} \sum_{i=1}^n (y_i - \hat{f}_M(x_i))^2 (1 - C(M)/n)^2 \quad (6)$$

$C(M)$ refers to complexity penalty, which depends on the number of basic functions and can be obtained (Chou et al., [2004](#); De Cos Juez et al., [2009](#); Friedman & Roosen, [1995](#); Nieto & Antón, [2014](#); Nieto et al., [2012](#), [2011](#); Orhan et al., [2011](#); Xu et al., [2004](#)) as:

$C(M) = (M+1) + dM$ (7) M refers to the number of functions used as basic in Equation (5); d indicates a penalty for the basic functions utilized in the proposed model. Increase in the value of d causes fewer required basic functions and smoother estimation.

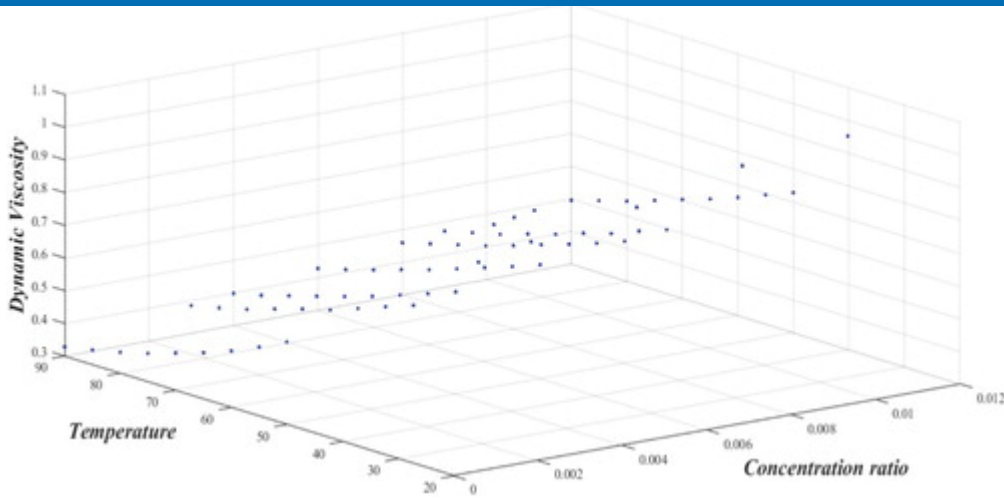
When the MARS model is generated, the importance of the utilized variables for modeling can be assessed. Taking into account the literatures several criteria can be applied which in this study, the GCV parameter is used for this purpose to achieve reliable results (Chou et al., [2004](#); De Cos Juez et al., [2009](#); Friedman & Roosen, [1995](#); Nieto & Antón, [2014](#); Nieto et al., [2012](#), [2011](#); Orhan et al., [2011](#); Xu et al., [2004](#)).

3. Results and discussion

3.1. Multivariable polynomial regression

In this study, experimental results from previous publications are used to model the range of the input variables and represented in Table 1. The data used for the modeling step are taken from experiments that were published recently (Alade, Oyehan, Popoola, Olatunji, & Bagudu, [2018](#); Esfe, Saedodin, Biglari, & Rostamian, [2016](#); Nikkam & Toprak, [2018](#)). The temperature of the fluid and the concentration ratio of the Ag/water nanofluid are those major elements which considerably affect the value of dynamic viscosity as illustrated in Figure 2.

Figure 2. Dynamic viscosity of Ag/water versus concentration and temperature.



[Display full size](#)

Table 1. Ranges of input variables (Alade et al., 2018 ; Esfe et al., 2016 ; Nikkam & Toprak, 2018)

[Download CSV](#)

[Display Table](#)



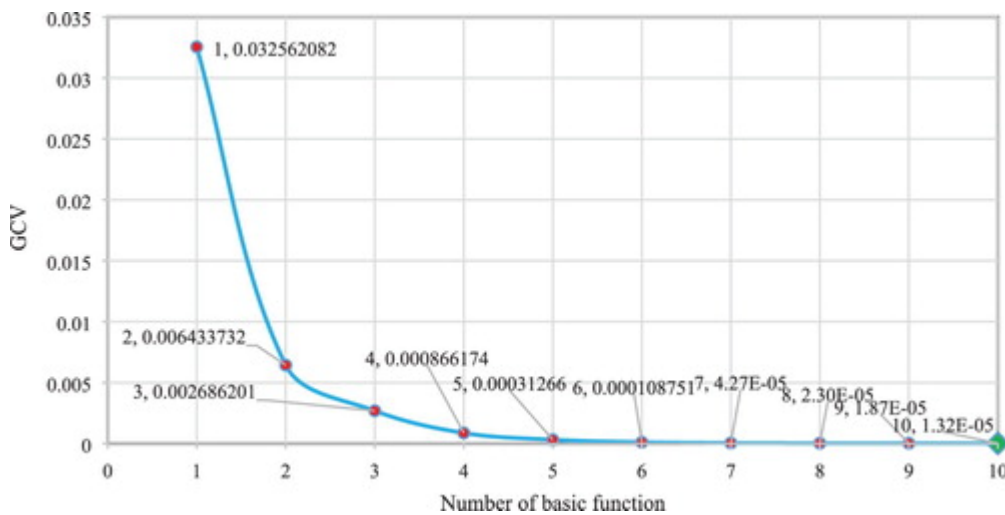
By using 2D multivariate polynomial regression and applying the least square method (Royston & Sauerbrei, 2008; Sinha, 2013), a simple equation is obtained for the experimental data that is represented in Alade et al. (2018), Esfe et al. (2016) and Nikkam and Toprak (2018). The proposed model has three inputs including temperature, size of nanoparticles and volumetric concentration. This model is very simple, lacking any exponential or logarithmic term. The complex models obtained by neural networks have some disadvantages such as high computational cost. The coefficients of the model are shown in Equation (8):

$$\mu = a_1 + a_2 \times T + a_3 \times \phi + a_4 \times d + a_5 \times T \times \phi + a_6 \times d \times T + a_7 \times d \times \phi + a_8 \times \phi^2 + a_9 \times T^2 \quad (8)$$

3.2. Multivariate adaptive regression splines

As mentioned earlier, in the MARS algorithm, the cores of procedure are basic functions; therefore, it is necessary to choose appropriate ones. Unlimited increase in the basic functions causes overfitting. In this study, the sensitivity of the MARS model based on the input basic functions is investigated. According to Jerome H. Friedman (1991), the GCV method is used to obtain the optimal number of functions in which using 10 basic functions leads to the best results (Figure 3). The coefficients of the proposed model in Equation (8) are reported in Table 2.

Figure 3. GCV versus number of basic functions.



Display full size

Table 2. Coefficients of the proposed models

Display Table



The model obtained using 10 basic functions is represented in Equation (9). The coefficients of the proposed model in Equation (9) are reported in Table 2.

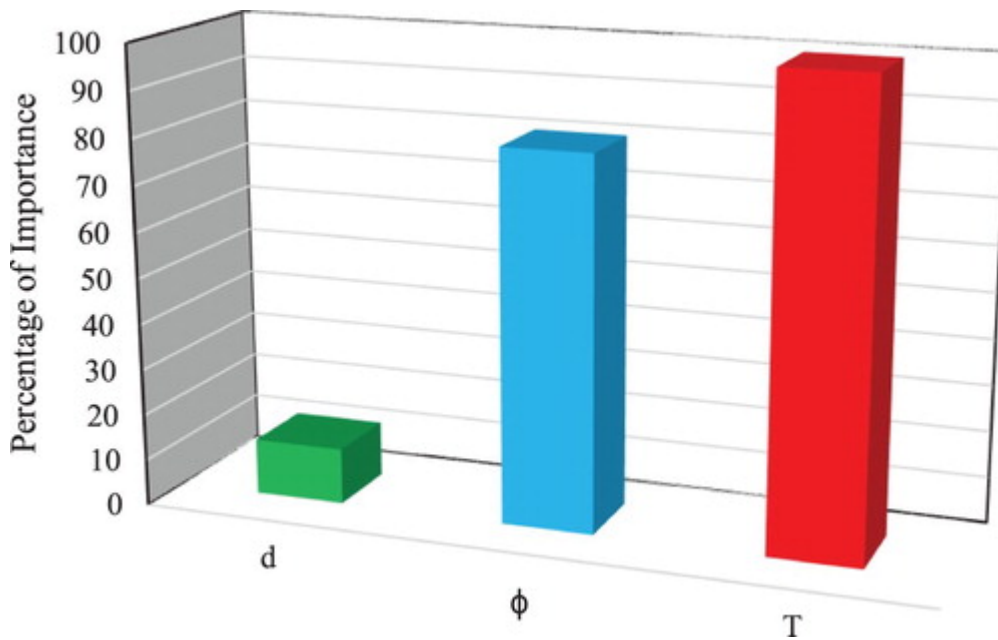
$$\mu = b_7 + b_8 \times BF_1 + b_9 \times BF_2 + b_{10} \times BF_3 + b_{11} \times BF_4 + b_{12} \times BF_5 + b_{13} \times BF_6 + b_{14} \times BF_7 + b_{15} \times BF_8 + b_{16} \times BF_9 + b_{17} \times BF_{10} \quad (9)$$

$$BF_1 = \text{Max}(0, T - b_1); BF_2 = \text{Max}(0, b_1 - T); BF_3 = \text{Max}(0, \varphi - b_2); BF_4 = \text{Max}(0, b_2 - \varphi); BF_5 = \text{Max}(0, b_3 - d); BF_6 = \text{Max}(0, b_4 - T); BF_7 = BF_5 \times \text{Max}(0, b_2 - \varphi); BF_8 = BF_1 \times \text{Max}(0, \varphi - b_5); BF_9 = BF_1 \times \text{Max}(0, b_5 - \varphi); BF_{10} = BF_4 \times \text{Max}(0, b_6 - T)$$

In most of the studies in which the MARS method is used for regression modeling, the importance of data is calculated for gaining better insight into the influential parameters. Data whose importance is equal to 0 will be removed.

In order for gaining the relative importance of one parameter, the root square of the GCV of the all basis function without involving the proposed parameter should be obtained and then the value must be scaled to 100. Based on importance data analysis, temperature has the most significant effect compared with temperature and concentration (Figure 4). The concentration of nanofluid has the second rank in the calculation of dynamic viscosity.

Figure 4. Importance of input variables.

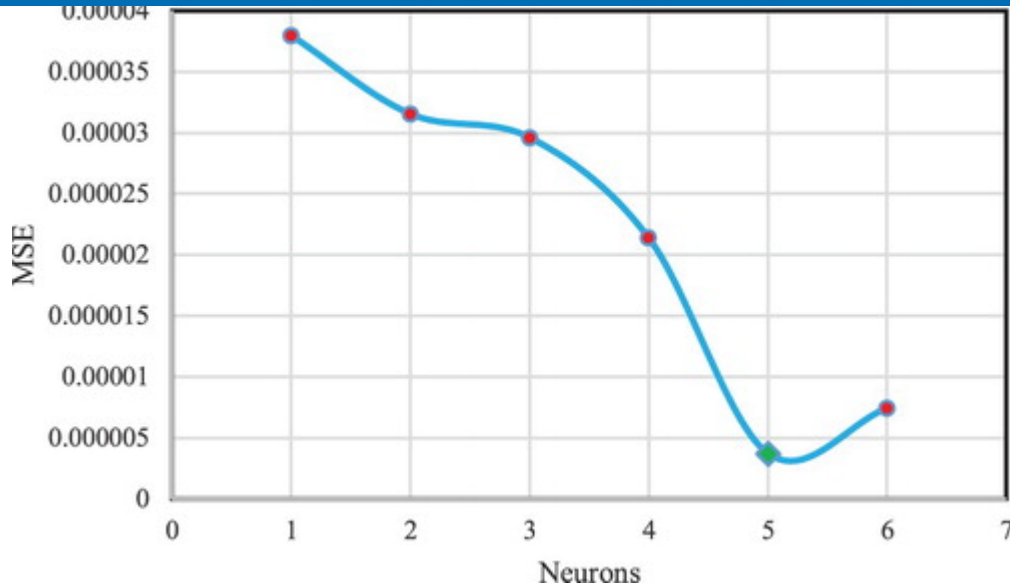


[Display full size](#)

3.3. MLP-LMA: feed-forward back propagation with Levenberg-Marquardt training Algorithm

In MLP neural networks, hidden layers and their neurons play the key role in regression. Inappropriate model selection and an inadequate number of layers and neurons lead to unfavorable outputs. Therefore, it is necessary to analyze the sensitivity of the network to the number of neurons and hidden layers. Since there are three input variables, a hidden layer is appropriate to obtain acceptable training; however, the sensitivity of the network must be considered based on the number of neurons. In the present study, MSE is used as a criterion to select the optimum number of neurons. As shown in Figure 5, using 5 neurons leads to the best model.

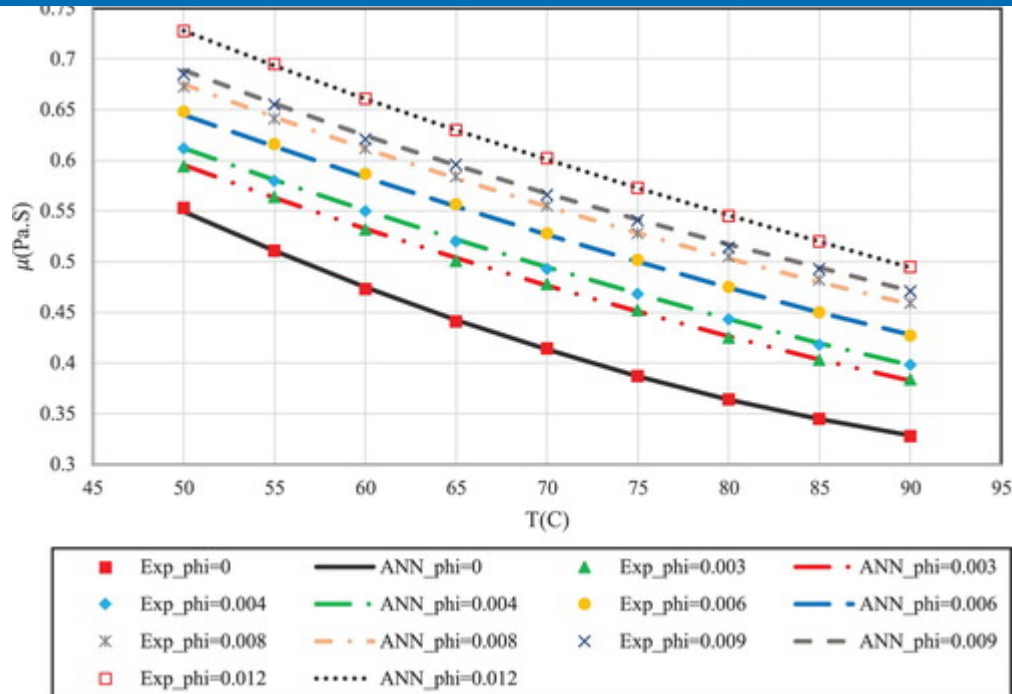
Figure 5. MSE value for various number of neurons.



[Display full size](#)

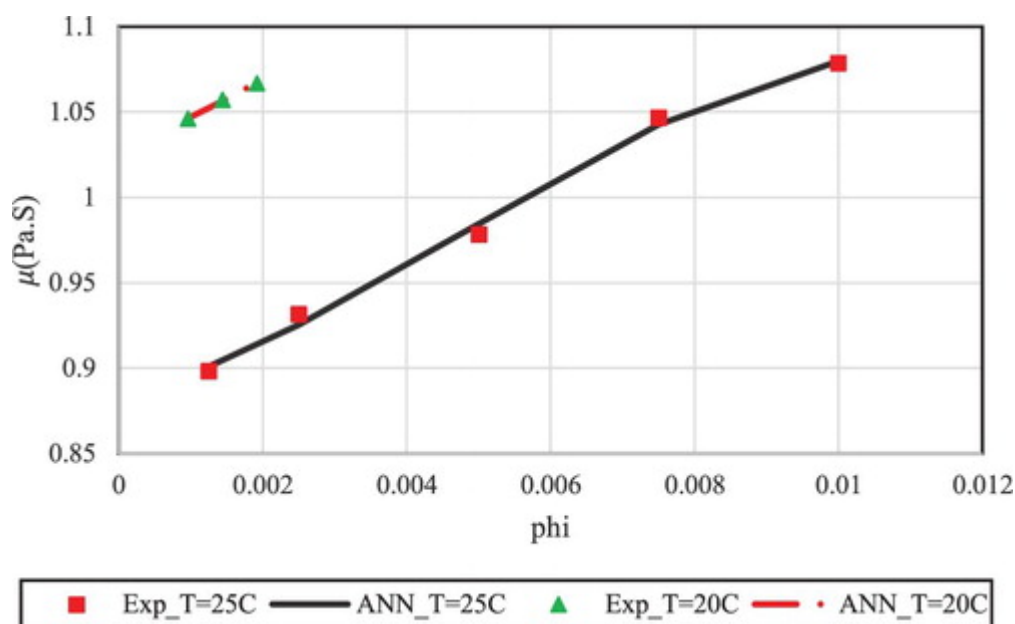
Neural Network identifier: 75% of data were used for training the network, 15% for validation and 10% for testing the trained network. The activation function for the hidden layer was tanh and an identity function was utilized for the output layer. The best model of the ANN was obtained in epoch 197 on the basis of MSE. In Figures 6 and 7 are represented the calculated dynamic viscosities of the nanofluid based on the concentration and temperature. Figure 6 represents the dynamic viscosity of Ag/water nanofluid in seven concentrations including 0, 0.003, 0.004, 0.006, 0.008, 0.009 and 0.012 in the temperature range of 50–90°C. The average size of nanoparticles in these cases equals 63 nm. As has been shown, an increase in temperature leads to higher dynamic viscosity for each temperature. In addition, it can be concluded that higher temperature causes lower dynamic viscosity for a constant concentration. For instance, increasing the temperature from 50 to 70°C in 0.003 concentration leads to approximately 19.5% reduction in dynamic viscosity.

Figure 6 Dynamic viscosity of Ag/water nanofluid in different temperatures and concentrations.



[Display full size](#)

Figure 7. Dynamic viscosity of Ag/water nanofluid versus temperature and concentration.



[Display full size](#)

In Figure 7 is represented the dynamic viscosity of Ag/water nanofluid in 20 and 25°C for particle size equal to 40 nm. The concentrations of the solid phase in these conditions are in the range of 0.00096 and 0.01. As illustrated, an increase in concentration, with constant temperature and particle size, results in improvement in dynamic viscosity; while a temperature increase reduces the dynamic viscosity.

3.4. Statistical comparison of the proposed models

$$AAPRE\% = \frac{\sum_{i=1}^n |t_i - o_i|}{\sum_{i=1}^n t_i} \times 100$$
 (Average Absolute Percent Relative Error)


$$RMSE = \sqrt{\frac{1}{n} \sum_{i=1}^n (t_i - o_i)^2}$$
 (Root Mean Square Error)

$$R^2 = 1 - \frac{\sum_{i=1}^n (t_i - o_i)^2}{\sum_{i=1}^n (t_i - t_m)^2}, t_m = \frac{\sum_{i=1}^n t_i}{n}$$
 (Coefficient of determination)

Based on the statistical criteria for regression evaluation (Baghban, Kahani, Nazari, Ahmadi, & Yan, [2019](#); Hajikhodaverdikhan, Nazari, Mohsenizadeh, Shamshirband, & Chau, [2018](#); Taormina, Chau, & Sivakumar, [2015](#); Wu & Chau, [2011](#)), the MLP network is the best among the approaches represented in the present study for modeling the dynamic viscosity of Ag/water nanofluid; however, using this algorithm requires more computational cost than does polynomial regression. A summary of the results obtained for each algorithm is presented in Table 3.

Table 3. Statistical comparison of various models

Display Table



4. Conclusion

In the present study, MLP and MARS algorithms were employed to estimate the dynamic viscosity of Ag/water nanofluid by considering nanoparticles' size and concentration and the temperature of the fluid as input variables. The value of R^2 was used as a statistical benchmark to evaluate the obtained outcomes. According to the calculations, the R^2 values for ANN-MLP, MARS and MPR algorithms were equal to 0.9998, 0.9997 and 0.9996, respectively in which conforming to the all statistical criterias describe in [Table 3](#), the proposed ANN-MLP is better than the two other algorithms. It could be concluded that all the applied algorithms are appropriate for modeling and able to precisely predict the dynamic viscosity of the nanofluid. In addition, the relative importance of the input data was determined to get better insight into the influential factors. Based on the obtained values, the importance of temperature, concentration and size was approximately 100%, 80% and 12%, respectively. These values indicate the high importance of temperature in modeling the dynamic viscosity.

Disclosure statement

No potential conflict of interest was reported by the authors.

Related Research Data

[Rainfall-runoff modeling using artificial neural network coupled with singular spectrum analysis](#)

Source: Journal of Hydrology

[Study of cyanotoxins presence from experimental cyanobacteria concentrations using a new data mining methodology based on multivariate adaptive regression splines in Trasona reservoir \(Northern Spain\)](#)

Source: Journal of Hazardous Materials

[Fabrication and thermo-physical characterization of silver nanofluids: An experimental investigation on the effect of base liquid](#)

Source: International Communications in Heat and Mass Transfer

[Applying GMDH artificial neural network in modeling CO2 emissions in four nordic countries](#)

Source: International Journal of Low-Carbon Technologies

[Applicability of connectionist methods to predict thermal resistance of](#)

References

1. Ahmadi, M.-A., Ahmadi, M. H., Alavi, M. F., Nazemzadegan, M. R., Ghasempour, R., & Shamshirband, S. (2018). Determination of thermal conductivity ratio of CuO/ethylene glycol nanofluid by connectionist approach. Journal of the Taiwan Institute of Chemical Engineers, 91, 383–395.

[Web of Science ®](#) | [Google Scholar](#)

2. Ahmadi, M. H., Ahmadi, M. A., Nazari, M. A., Mahian, O., & Ghasempour, R. (2018). A proposed model to predict thermal conductivity ratio of Al₂O₃/EG nanofluid by

applying least squares support vector machine (LSSVM) and genetic algorithm as a connectionist approach. *Journal of Thermal Analysis and Calorimetry*, 1-11.

[Web of Science ®](#) | [Google Scholar](#)

3. Ahmadi, M. H., Mirlohi, A., Nazari, M. A., & Ghasempour, R. (2018). A review of thermal conductivity of various nanofluids. *Journal of Molecular Liquids*, 265, 181-188.

[Web of Science ®](#) | [Google Scholar](#)

4. Ahmadi, M. H., Tatar, A., Nazari, M. A., Ghasempour, R., Chamkha, A. J., & Yan, W.-M. (2018). Applicability of connectionist methods to predict thermal resistance of pulsating heat pipes with ethanol by using neural networks. *International Journal of Heat and Mass Transfer*, 126, 1079-1086.

[Web of Science ®](#) | [Google Scholar](#)

5. Ahmadi, M. H., Tatar, A., Seifaddini, P., Ghazvini, M., Ghasempour, R., & Sheremet, M. A. (2018). Thermal conductivity and dynamic viscosity modeling of Fe₂O₃/water nanofluid by applying various connectionist approaches. *Numerical Heat Transfer, Part A: Applications*, 74, 1-22.

[Web of Science ®](#) | [Google Scholar](#)

6. Alade, I. O., Oyehan, T. A., Popoola, I. K., Olatunji, S. O., & Bagudu, A. (2018). Modeling thermal conductivity enhancement of metal and metallic oxide nanofluids using support vector regression. *Advanced Powder Technology*, 29(1), 157-167.

[Web of Science ®](#) | [Google Scholar](#)

7. Asadi, M., & Asadi, A. (2016). Dynamic viscosity of MWCNT/ZnO-engine oil hybrid nanofluid: An experimental investigation and new correlation in different temperatures and solid concentrations. *International Communications in Heat and Mass Transfer*, 76, 41-45.

[Web of Science ®](#) | [Google Scholar](#)

8. Baghban, A., Jalali, A., Shafiee, M., Ahmadi, M. H., & Chau, K.-W. (2019). Developing an ANFIS-based swarm concept model for estimating the relative viscosity of nanofluids. *Engineering Applications of Computational Fluid Mechanics*, 13(1), 26–39.

[Web of Science ®](#) | [Google Scholar](#)

9. Baghban, A., Kahani, M., Nazari, M. A., Ahmadi, M. H., & Yan, W.-M. (2019). Sensitivity analysis and application of machine learning methods to predict the heat transfer performance of CNT/water nanofluid flows through coils. *International Journal of Heat and Mass Transfer*, 128, 825–835.

[Web of Science ®](#) | [Google Scholar](#)

10. Baghban, A., Pourfayaz, F., Ahmadi, M. H., Kasaeian, A., Pourkiaei, S. M., & Lorenzini, G. (2018). Connectionist intelligent model estimates of convective heat transfer coefficient of nanofluids in circular cross-sectional channels. *Journal of Thermal Analysis and Calorimetry*, 132(2), 1213–1239.

[Web of Science ®](#) | [Google Scholar](#)

11. Chau, K.-W. (2017). Use of meta-heuristic techniques in rainfall-runoff modelling. Multidisciplinary Digital Publishing Institute, 186.

[Google Scholar](#)

12. Chiam, H., Azmi, W., Usri, N., Mamat, R., & Adam, N. (2017). Thermal conductivity and viscosity of Al₂O₃ nanofluids for different based ratio of water and ethylene glycol mixture. *Experimental Thermal and Fluid Science*, 81, 420–429.

[Web of Science ®](#) | [Google Scholar](#)

13. Chou, S.-M., Lee, T.-S., Shao, Y. E., & Chen, I.-F. (2004). Mining the breast cancer pattern using artificial neural networks and multivariate adaptive regression splines. *Expert Systems with Applications*, 27(1), 133–142.

[Web of Science ®](#) | [Google Scholar](#)

14. De Cos Juez, F. J., Lasheras, F. S., García Nieto, P. J., & Suárez, M. S. (2009). A new

lifestyle on the value of bone mineral density in post-menopausal women.

International Journal of Computer Mathematics, 86(10-11), 1878-1887.

[Web of Science ®](#) | [Google Scholar](#)

5. Ebrahimi-Moghadam, A., Mohseni-Gharyehsafa, B., & Farzaneh-Gord, M. (2018). Using artificial neural network and quadratic algorithm for minimizing entropy generation of Al₂O₃-EG/W nanofluid flow inside parabolic trough solar collector. *Renewable Energy*, 129, 473-485.

[Web of Science ®](#) | [Google Scholar](#)

6. Esfe, M. H., Saedodin, S., Biglari, M., & Rostamian, H. (2016). An experimental study on thermophysical properties and heat transfer characteristics of low volume concentrations of Ag-water nanofluid. *International Communications in Heat and Mass Transfer*, 74, 91-97.

[Web of Science ®](#) | [Google Scholar](#)

7. Friedman, J. H. (1991). Multivariate adaptive regression splines. *The Annals of Statistics*, 19, 1-67.

[Web of Science ®](#) | [Google Scholar](#)

8. Friedman, J. H., & Roosen, C. B. (1995). An introduction to multivariate adaptive regression splines. *Statistical Methods in Medical Research*, 4, 197-217.

[PubMed](#) | [Google Scholar](#)

9. Gardner, M. W., & Dorling, S. (1998). Artificial neural networks (the multilayer perceptron)—a review of applications in the atmospheric sciences. *Atmospheric Environment*, 32(14-15), 2627-2636.

[Web of Science ®](#) | [Google Scholar](#)

10. Goda, H. M., Shokir, E.-M., Eissa, M., Fattah, K. A., & Sayyoun, M. H. (2003). Prediction of the PVT data using neural network computing theory. Nigeria annual international conference and exhibition.

21. Hajikhodaverdikhan, P., Nazari, M., Mohsenizadeh, M., Shamshirband, S., & Chau, K.-W. (2018). Earthquake prediction with meteorological data by particle filter-based support vector regression. *Engineering Applications of Computational Fluid Mechanics*, 12(1), 679–688.

[Web of Science ®](#) | [Google Scholar](#)

22. Hornik, K., Stinchcombe, M., & White, H. (1989). Multilayer feedforward networks are universal approximators. *Neural Networks*, 2(5), 359–366.

[Web of Science ®](#) | [Google Scholar](#)

23. Hosseini, F., Kasaeian, A., Pourfayaz, F., Sheikhpour, M., & Wen, D. (2018). Novel ZnO-Ag/MWCNT nanocomposite for the photocatalytic degradation of phenol. *Materials Science in Semiconductor Processing*, 83, 175–185.

[Web of Science ®](#) | [Google Scholar](#)

24. Kazemi, S., Minaei Bidgoli, B., Shamshirband, S., Karimi, S. M., Ghorbani, M. A., Chau, K.-W., & Kazem Pour, R. (2018). Novel genetic-based negative correlation learning for estimating soil temperature. *Engineering Applications of Computational Fluid Mechanics*, 12(1), 506–516.

[Web of Science ®](#) | [Google Scholar](#)

25. Mohseni-Gharyehsafa, B., Ebrahimi-Moghadam, A., Okati, V., Farzaneh-Gord, M., Ahmadi, M. H., & Lorenzini, G. (2018). Optimizing flow properties of the different nanofluids inside a circular tube by using entropy generation minimization approach. *Journal of Thermal Analysis and Calorimetry*, 1–11.

[Web of Science ®](#) | [Google Scholar](#)

26. Nazari, M. A., Ahmadi, M. H., Ghasempour, R., & Shafii, M. B. (2018). How to improve the thermal performance of pulsating heat pipes: A review on working fluid. *Renewable and Sustainable Energy Reviews*, 91, 630–638.

[Web of Science ®](#) | [Google Scholar](#)

17. Nazari, M. A., Ghasempour, R., Ahmadi, M. H., Heydarian, G., & Shafii, M. B. (2018). Experimental investigation of graphene oxide nanofluid on heat transfer enhancement of pulsating heat pipe. *International Communications in Heat and Mass Transfer*, 91, 90–94.

[Web of Science ®](#) | [Google Scholar](#)

18. Nieto, P. G., & Antón, J.Á. (2014). Nonlinear air quality modeling using multivariate adaptive regression splines in Gijón urban area (Northern Spain) at local scale. *Applied Mathematics and Computation*, 235, 50–65.

[Web of Science ®](#) | [Google Scholar](#)

19. Nieto, P. G., Fernández, J. A., Lasheras, F. S., de Cos Juez, F., & Muñiz, C. D. (2012). A new improved study of cyanotoxins presence from experimental cyanobacteria concentrations in the Trasona reservoir (Northern Spain) using the MARS technique. *Science of the Total Environment*, 430, 88–92.

[PubMed](#) | [Web of Science ®](#) | [Google Scholar](#)

20. Nieto, P. G., García-Gonzalo, E., Bernardo Sanchez, A., & Menendez Fernandez, M. (2016). A new predictive model based on the ABC optimized multivariate adaptive regression splines approach for predicting the remaining useful life in aircraft engines. *Energies*, 9(6), 88–92.

[Web of Science ®](#) | [Google Scholar](#)

21. Nieto, P. G., Lasheras, F. S., de Cos Juez, F., & Fernández, J. A. (2011). Study of cyanotoxins presence from experimental cyanobacteria concentrations using a new data mining methodology based on multivariate adaptive regression splines in Trasona reservoir (Northern Spain). *Journal of Hazardous Materials*, 195, 414–421.

[PubMed](#) | [Web of Science ®](#) | [Google Scholar](#)

22. Nikkam, N., & Toprak, M. S. (2018). Fabrication and thermo-physical characterization of silver nanofluids: An experimental investigation on the effect of base liquid. *International Communications in Heat and Mass Transfer*, 91, 196–200.

33. Orhan, U., Hekim, M., & Ozer, M. (2011). EEG signals classification using the K-means clustering and a multilayer perceptron neural network model. *Expert Systems with Applications*, 38(10), 13475–13481.

[Web of Science ®](#) | [Google Scholar](#)

34. Ramezanizadeh, M., Alhuyi Nazari, M., Ahmadi, M. H., & Chau, K.-W. (2019). Experimental and numerical analysis of a nanofluidic thermosyphon heat exchanger. *Engineering Applications of Computational Fluid Mechanics*, 13(1), 40–47.

[Web of Science ®](#) | [Google Scholar](#)

35. Rezaei, M. H., Sadeghzadeh, M., Alhuyi Nazari, M., Ahmadi, M. H., & Astarai, F. R. (2018). Applying GMDH artificial neural network in modeling CO₂ emissions in four nordic countries. *International Journal of Low-Carbon Technologies*, 13(3), 266–271.

[Web of Science ®](#) | [Google Scholar](#)

36. Royston, P., & Sauerbrei, W. (2008). *Multivariable model-building: A pragmatic approach to regression analysis based on fractional polynomials for modelling continuous variables* (Vol. 777). London: John Wiley & Sons.

[Google Scholar](#)

37. Ruck, D. W., Rogers, S. K., Kabrisky, M., Oxley, M. E., & Suter, B. W. (1990). The multilayer perceptron as an approximation to a Bayes optimal discriminant function. *IEEE Transactions on Neural Networks*, 1(4), 296–298.

[PubMed](#) | [Google Scholar](#)

38. Saidur, R., Leong, K., & Mohammad, H. (2011). A review on applications and challenges of nanofluids. *Renewable and Sustainable Energy Reviews*, 15(3), 1646–1668.

[Web of Science ®](#) | [Google Scholar](#)

39. Sinha, P. (2013). Multivariate polynomial regression in data mining: Methodology, problems and solutions. *International Journal of Scientific and Engineering Research*,

40. Soltani, O., & Akbari, M. (2016). Effects of temperature and particles concentration on the dynamic viscosity of MgO-MWCNT/ethylene glycol hybrid nanofluid: Experimental study. *Physica E: Low-Dimensional Systems and Nanostructures*, 84, 564–570.

[Web of Science ®](#) | [Google Scholar](#)

41. Taormina, R., Chau, K.-W., & Sivakumar, B. (2015). Neural network river forecasting through baseflow separation and binary-coded swarm optimization. *Journal of Hydrology*, 529, 1788–1797.

[Web of Science ®](#) | [Google Scholar](#)

42. Vanzella, E., Cristiani, S., Fontana, A., Nonino, M., Arnouts, S., Giallongo, E., ... Zaggia, S. (2004). Photometric redshifts with the multilayer perceptron neural network: Application to the HDF-S and SDSS. *Astronomy & Astrophysics*, 423(2), 761–776.

[Web of Science ®](#) | [Google Scholar](#)

43. Vasanthakumari, R., & Pondy, P. (2018). Mixed convection of silver and titanium dioxide nanofluids along inclined stretching sheet in presence of MHD with heat generation and suction effect. *Mathematical Modelling of Engineering Problems*, 5(2), 123–129.

[Google Scholar](#)

44. Wang, X.-H., & Jiao, Y.-L. (2015). Study on the heat transfer characteristic of heat pipe containing magnetic nano-fluids strengthened by magnetic field. *International Journal of Heat and Technology*, 33(1), 137–144.

[Google Scholar](#)

45. Wu, C., & Chau, K. (2011). Rainfall-runoff modeling using artificial neural network coupled with singular spectrum analysis. *Journal of Hydrology*, 399(3-4), 394–409.

[Web of Science ®](#) | [Google Scholar](#)

6. Xu, Q.-S., Daszykowski, M., Walczak, B., Daeyaert, F., De Jonge, M., Heeres, J., ...
Massart, D. L. (2004). Multivariate adaptive regression splines—studies of HIV reverse
transcriptase inhibitors. *Chemometrics and Intelligent Laboratory Systems*, 72(1), 27–
34.

[Web of Science ®](#) | [Google Scholar](#)

7. Zeinali Heris, S., Kazemi-Beydokhti, A., Noie, S., & Rezvan, S. (2012). Numerical study
on convective heat transfer of Al₂O₃/water, CuO/water and Cu/water nanofluids
through square cross-section duct in laminar flow. *Engineering Applications of
Computational Fluid Mechanics*, 6(1), 1–14.

[Web of Science ®](#) | [Google Scholar](#)

[Download PDF](#)

Related research

People also read

Recommended articles

Cited by
39

Information for

Authors
R&D professionals
Editors
Librarians
Societies

Opportunities

Reprints and e-prints
Advertising solutions
Accelerated publication
Corporate access solutions

Open access

Overview
Open journals
Open Select
Dove Medical Press
F1000Research

Help and information

Help and contact
Newsroom
All journals
Books

Keep up to date

Register to receive personalised research and resources by email

 Sign me up



Copyright © 2025 Informa UK Limited Privacy policy Cookies Terms & conditions
Accessibility

Registered in England & Wales No. 01072954
5 Howick Place | London | SW1P 1WG

